

Event-plane dependent dihadron correlations with harmonic v_n subtraction in Au+Au Collisions at $\sqrt{s_{NN}} = 200$ GeV

H. Agakishiev,¹⁷ M. M. Aggarwal,²⁹ Z. Ahammed,²¹ A. V. Alakhverdyants,¹⁷ I. Alekseev,¹⁵ J. Alford,¹⁸ B. D. Anderson,¹⁸ C. D. Anson,²⁷ D. Arkhipkin,² G. S. Averichev,¹⁷ J. Balewski,²² D. R. Beavis,² N. K. Behera,¹³ R. Bellwied,⁴⁹ M. J. Betancourt,²² R. R. Betts,⁷ A. Bhasin,¹⁶ A. K. Bhati,²⁹ H. Bichsel,⁴⁸ J. Bielcik,⁹ J. Bielcikova,¹⁰ B. Biritz,⁵ L. C. Bland,² W. Borowski,⁴⁰ J. Bouchet,¹⁸ E. Braidot,²⁶ A. V. Brandin,²⁵ A. Bridgeman,¹ S. G. Brovko,⁴ E. Bruna,⁵¹ S. Bueltmann,²⁸ I. Bunzarov,¹⁷ T. P. Burton,² X. Z. Cai,³⁹ H. Caines,⁵¹ M. Calderón de la Barca Sánchez,⁴ D. Cebra,⁴ R. Cendejas,⁵ M. C. Cervantes,⁴¹ Z. Chajecski,²⁷ P. Chaloupka,¹⁰ S. Chattopadhyay,⁴⁶ H. F. Chen,³⁷ J. H. Chen,³⁹ J. Y. Chen,⁵⁰ L. Chen,⁵⁰ J. Cheng,⁴³ M. Cherney,⁸ A. Chikanian,⁵¹ K. E. Choi,³³ W. Christie,² P. Chung,¹⁰ M. J. M. Coddington,⁴¹ R. Corliss,²² J. G. Cramer,⁴⁸ H. J. Crawford,³ S. Dash,¹² A. Davila Leyva,⁴² L. C. De Silva,⁴⁹ R. R. Debbes,² T. G. Dedovich,¹⁷ A. A. Derevschikov,³¹ R. Derradi de Souza,⁶ L. Didenko,² P. Djawotho,⁴¹ S. M. Dogra,¹⁶ X. Dong,²¹ J. L. Drachenberg,⁴¹ J. E. Draper,⁴ J. C. Dunlop,² L. G. Efimov,¹⁷ M. Elmimr,⁴⁹ J. Engelage,³ G. Eppley,³⁵ M. Estienne,⁴⁰ L. Eun,³⁰ O. Evdokimov,⁷ R. Fatemi,¹⁹ J. Fedorisin,¹⁷ A. Feng,⁵⁰ R. G. Fersch,¹⁹ P. Filip,¹⁷ E. Finch,⁵¹ V. Fine,² Y. Fisyak,² C. A. Gagliardi,⁴¹ D. R. Gangadharan,⁵ A. Geromitsos,⁴⁰ F. Geurts,³⁵ P. Ghosh,⁴⁶ Y. N. Gorbunov,⁸ A. Gordon,² O. Grebenyuk,²¹ D. Grosnick,⁴⁵ S. M. Guertin,⁵ A. Gupta,¹⁶ W. Guryn,² B. Haag,⁴ O. Hajkova,⁹ A. Hamed,⁴¹ L-X. Han,³⁹ J. W. Harris,⁵¹ J. P. Hays-Wehle,²² M. Heinz,⁵¹ S. Heppelmann,³⁰ A. Hirsch,³² E. Hjort,²¹ G. W. Hoffmann,⁴² D. J. Hofman,⁷ B. Huang,³⁷ H. Z. Huang,⁵ T. J. Humanic,²⁷ L. Huo,⁴¹ G. Igo,⁵ P. Jacobs,²¹ W. W. Jacobs,¹⁴ C. Jena,¹² F. Jin,³⁹ J. Joseph,¹⁸ E. G. Judd,³ S. Kabana,⁴⁰ K. Kang,⁴³ J. Kapitan,¹⁰ K. Kauder,⁷ H. Ke,⁵⁰ D. Keane,¹⁸ A. Kechechyan,¹⁷ D. Kettler,⁴⁸ D. P. Kikola,²¹ J. Kiryluk,²¹ A. Kisiel,⁴⁷ V. Kizka,¹⁷ A. G. Knospe,⁵¹ D. D. Koetke,⁴⁵ T. Kollegger,¹¹ J. Konzer,³² I. Koralt,²⁸ L. Koroleva,¹⁵ W. Korsch,¹⁹ L. Kotchenda,²⁵ V. Kouchpil,¹⁰ P. Kravtsov,²⁵ K. Krueger,¹ M. Krus,⁹ L. Kumar,¹⁸ P. Kurnadi,⁵ M. A. C. Lamont,² J. M. Landgraf,² S. LaPointe,⁴⁹ J. Lauret,² A. Lebedev,² R. Lednický,¹⁷ J. H. Lee,² W. Leight,²² M. J. LeVine,² C. Li,³⁷ L. Li,⁴² N. Li,⁵⁰ W. Li,³⁹ X. Li,³² X. Li,³⁸ Y. Li,⁴³ Z. M. Li,⁵⁰ M. A. Lisa,²⁷ F. Liu,⁵⁰ H. Liu,⁴ J. Liu,³⁵ T. Ljubicic,² W. J. Llope,³⁵ R. S. Longacre,² W. A. Love,² Y. Lu,³⁷ E. V. Lukashov,²⁵ X. Luo,³⁷ G. L. Ma,³⁹ Y. G. Ma,³⁹ D. P. Mahapatra,¹² R. Majka,⁵¹ O. I. Mall,⁴ L. K. Mangotra,¹⁶ R. Manweiler,⁴⁵ S. Margetis,¹⁸ C. Markert,⁴² H. Masui,²¹ H. S. Matis,²¹ Yu. A. Matulenko,³¹ D. McDonald,³⁵ T. S. McShane,⁸ A. Meschanin,³¹ R. Milner,²² N. G. Minaev,³¹ S. Mioduszewski,⁴¹ A. Mischke,²⁶ M. K. Mitrovski,¹¹ B. Mohanty,⁴⁶ M. M. Mondal,⁴⁶ B. Morozov,¹⁵ D. A. Morozov,³¹ M. G. Munhoz,³⁶ M. Naglis,²¹ B. K. Nandi,¹³ T. K. Nayak,⁴⁶ P. K. Netrakanti,³² L. V. Nogach,³¹ S. B. Nurushev,³¹ G. Odyniec,²¹ A. Ogawa,² Oh,³³ Ohlson,⁵¹ V. Okorokov,²⁵ E. W. Oldag,⁴² D. Olson,²¹ M. Pachr,⁹ B. S. Page,¹⁴ S. K. Pal,⁴⁶ Y. Pandit,¹⁸ Y. Panebratsev,¹⁷ T. Pawlak,⁴⁷ H. Pei,⁷ T. Peitzmann,²⁶ C. Perkins,³ W. Peryt,⁴⁷ S. C. Phatak,¹² P. Pile,² M. Planinic,⁵² M. A. Ploskon,²¹ J. Pluta,⁴⁷ D. Plyku,²⁸ N. Poljak,⁵² A. M. Poskanzer,²¹ B. V. K. S. Potukuchi,¹⁶ C. B. Powell,²¹ D. Prindle,⁴⁸ N. K. Pruthi,²⁹ P. R. Pujahari,¹³ J. Putschke,⁵¹ H. Qiu,²⁰ R. Raniwala,³⁴ S. Raniwala,³⁴ R. Redwine,²² R. Reed,⁴ H. G. Ritter,²¹ J. B. Roberts,³⁵ O. V. Rogachevskiy,¹⁷ J. L. Romero,⁴ A. Rose,²¹ L. Ruan,² J. Rusnak,¹⁰ N. R. Sahoo,⁴⁶ S. Sakai,²¹ I. Sakrejda,²¹ T. Sakuma,²² S. Salur,⁴ J. Sandweiss,⁵¹ E. Sangaline,⁴ A. Sarkar,¹³ J. Schambach,⁴² R. P. Scharenberg,³² A. M. Schmah,²¹ N. Schmitz,²³ T. R. Schuster,¹¹ J. Seele,²² J. Seger,⁸ I. Selyuzhenkov,¹⁴ P. Seyboth,²³ E. Shahaliev,¹⁷ M. Shao,³⁷ M. Sharma,⁴⁹ S. S. Shi,⁵⁰ Q. Y. Shou,³⁹ E. P. Sichtermann,²¹ F. Simon,²³ R. N. Singaraju,⁴⁶ M. J. Skoby,³² N. Smirnov,⁵¹ H. M. Spinka,¹ B. Srivastava,³² T. D. S. Stanislaus,⁴⁵ D. Staszak,⁵ S. G. Steadman,²² J. R. Stevens,¹⁴ R. Stock,¹¹ M. Strikhanov,²⁵ B. Stringfellow,³² A. A. P. Suaide,³⁶ M. C. Suarez,⁷ N. L. Subba,¹⁸ M. Sumera,¹⁰ X. M. Sun,²¹ Y. Sun,³⁷ Z. Sun,²⁰ B. Surrow,²² D. N. Svirida,¹⁵ T. J. M. Symons,²¹ A. Szanto de Toledo,³⁶ J. Takahashi,⁶ A. H. Tang,² Z. Tang,³⁷ L. H. Tarini,⁴⁹ T. Tarnowsky,²⁴ D. Thein,⁴² J. H. Thomas,²¹ J. Tian,³⁹ A. R. Timmins,⁴⁹ D. Tlusty,¹⁰ M. Tokarev,¹⁷ V. N. Tram,²¹ S. Trentalange,⁵ R. E. Tribble,⁴¹ Tribedy,⁴⁶ O. D. Tsai,⁵ T. Ullrich,² D. G. Underwood,¹ G. Van Buren,² G. van Nieuwenhuizen,²² J. A. Vanfossen, Jr.,¹⁸ R. Varma,¹³ G. M. S. Vasconcelos,⁶ A. N. Vasiliev,³¹ F. Videbæk,² Y. P. Viyogi,⁴⁶ S. Vokal,¹⁷ M. Wada,⁴² M. Walker,²² F. Wang,³² G. Wang,⁵ H. Wang,²⁴ J. S. Wang,²⁰ Q. Wang,³² X. L. Wang,³⁷ Y. Wang,⁴³ G. Webb,¹⁹ J. C. Webb,² G. D. Westfall,²⁴ C. Whitten Jr.,⁵ H. Wieman,²¹ S. W. Wissink,¹⁴ R. Witt,⁴⁴ W. Witzke,¹⁹ Y. F. Wu,⁵⁰ Xiao,⁴³ W. Xie,³² H. Xu,²⁰ N. Xu,²¹ Q. H. Xu,³⁸ W. Xu,⁵ Y. Xu,³⁷ Z. Xu,² L. Xue,³⁹ Y. Yang,²⁰ P. Yepes,³⁵ K. Yip,² I-K. Yoo,³³ M. Zawisza,⁴⁷ H. Zbroszczyk,⁴⁷ W. Zhan,²⁰ J. B. Zhang,⁵⁰ S. Zhang,³⁹ W. M. Zhang,¹⁸ X. P. Zhang,⁴³ Y. Zhang,²¹ Z. P. Zhang,³⁷ J. Zhao,³⁹ C. Zhong,³⁹ W. Zhou,³⁸ X. Zhu,⁴³ Y. H. Zhu,³⁹ R. Zoulkarneev,¹⁷ and Y. Zoulkarneeva¹⁷

(STAR Collaboration)

- 1 ¹Argonne National Laboratory, Argonne, Illinois 60439, USA
2 ²Brookhaven National Laboratory, Upton, New York 11973, USA
3 ³University of California, Berkeley, California 94720, USA
4 ⁴University of California, Davis, California 95616, USA
5 ⁵University of California, Los Angeles, California 90095, USA
6 ⁶Universidade Estadual de Campinas, Sao Paulo, Brazil
7 ⁷University of Illinois at Chicago, Chicago, Illinois 60607, USA
8 ⁸Creighton University, Omaha, Nebraska 68178, USA
9 ⁹Czech Technical University in Prague, FNSPE, Prague, 115 19, Czech Republic
10 ¹⁰Nuclear Physics Institute AS CR, 250 68 Řež/Prague, Czech Republic
11 ¹¹University of Frankfurt, Frankfurt, Germany
12 ¹²Institute of Physics, Bhubaneswar 751005, India
13 ¹³Indian Institute of Technology, Mumbai, India
14 ¹⁴Indiana University, Bloomington, Indiana 47408, USA
15 ¹⁵Alikhanov Institute for Theoretical and Experimental Physics, Moscow, Russia
16 ¹⁶University of Jammu, Jammu 180001, India
17 ¹⁷Joint Institute for Nuclear Research, Dubna, 141 980, Russia
18 ¹⁸Kent State University, Kent, Ohio 44242, USA
19 ¹⁹University of Kentucky, Lexington, Kentucky, 40506-0055, USA
20 ²⁰Institute of Modern Physics, Lanzhou, China
21 ²¹Lawrence Berkeley National Laboratory, Berkeley, California 94720, USA
22 ²²Massachusetts Institute of Technology, Cambridge, MA 02139-4307, USA
23 ²³Max-Planck-Institut für Physik, Munich, Germany
24 ²⁴Michigan State University, East Lansing, Michigan 48824, USA
25 ²⁵Moscow Engineering Physics Institute, Moscow Russia
26 ²⁶NIKHEF and Utrecht University, Amsterdam, The Netherlands
27 ²⁷Ohio State University, Columbus, Ohio 43210, USA
28 ²⁸Old Dominion University, Norfolk, VA, 23529, USA
29 ²⁹Panjab University, Chandigarh 160014, India
30 ³⁰Pennsylvania State University, University Park, Pennsylvania 16802, USA
31 ³¹Institute of High Energy Physics, Protvino, Russia
32 ³²Purdue University, West Lafayette, Indiana 47907, USA
33 ³³Pusan National University, Pusan, Republic of Korea
34 ³⁴University of Rajasthan, Jaipur 302004, India
35 ³⁵Rice University, Houston, Texas 77251, USA
36 ³⁶Universidade de Sao Paulo, Sao Paulo, Brazil
37 ³⁷University of Science & Technology of China, Hefei 230026, China
38 ³⁸Shandong University, Jinan, Shandong 250100, China
39 ³⁹Shanghai Institute of Applied Physics, Shanghai 201800, China
40 ⁴⁰SUBATECH, Nantes, France
41 ⁴¹Texas A&M University, College Station, Texas 77843, USA
42 ⁴²University of Texas, Austin, Texas 78712, USA
43 ⁴³Tsinghua University, Beijing 100084, China
44 ⁴⁴United States Naval Academy, Annapolis, MD 21402, USA
45 ⁴⁵Valparaiso University, Valparaiso, Indiana 46383, USA
46 ⁴⁶Variable Energy Cyclotron Centre, Kolkata 700064, India
47 ⁴⁷Warsaw University of Technology, Warsaw, Poland
48 ⁴⁸University of Washington, Seattle, Washington 98195, USA
49 ⁴⁹Wayne State University, Detroit, Michigan 48201, USA
50 ⁵⁰Institute of Particle Physics, CCNU (HZNU), Wuhan 430079, China
51 ⁵¹Yale University, New Haven, Connecticut 06520, USA
52 ⁵²University of Zagreb, Zagreb, HR-10002, Croatia

STAR measurements of dihadron azimuthal correlations ($\Delta\phi$) are reported in mid-central (20-60%) Au+Au collisions at $\sqrt{s_{\text{NN}}} = 200$ GeV as a function of the trigger particle's azimuthal angle relative to the event plane, $\phi_s = |\phi_t - \psi_{\text{EP}}|$. The elliptic (v_2), triangular (v_3), and quadratic (v_4) flow harmonic backgrounds are subtracted using the Zero Yield At Minimum (ZYAM) method. The results are compared to minimum-bias d+Au collisions. It is found that a finite near-side ($|\Delta\phi| < \pi/2$) long-range pseudorapidity correlation (ridge) is present in the in-plane direction ($\phi_s \sim 0$). The away-side ($|\Delta\phi| > \pi/2$) correlation shows a modification from d+Au data, varying with ϕ_s . The modification may be a consequence of pathlength-dependent jet-quenching and may lead to a better understanding of high-density QCD.

The hot and dense QCD matter created in heavy-ion collisions at the Relativistic Heavy-Ion Collider (RHIC) of Brookhaven National Laboratory reveals properties of a nearly perfect fluid of strongly interacting quarks and gluons [1]. These properties include strong elliptical azimuthal emission as large as hydrodynamical prediction relative to the initial geometry eccentricity [2], and strong attenuation of high transverse momentum (p_T) particles due to jet-medium interactions (jet-quenching) [3, 4]. The energy lost at high p_T must be redistributed to lower p_T particles [5]. The distribution of those particles relative to a high- p_T trigger particle can therefore provide information about the nature of the QCD interactions.

The magnitude of the effect from jet-medium interactions should depend on the pathlength the jet traverses [3]. This pathlength dependence may be studied in non-central heavy-ion collisions [6], where the transverse overlap region between the two colliding nuclei is anisotropic. The short-axis direction of the overlap region may be estimated by the direction of the most probable particle emission [7]. The estimated direction together with the beam axis is called the event plane (EP), and is a proxy for the initial geometry participant plane (ψ_2) [8]. By selecting the trigger particle's azimuth relative to the event plane, $\phi_s = |\phi_t - \psi_{EP}|$, one effectively selects different average pathlengths through the medium that the away-side jet traverses, providing differential information unavailable to inclusive jet-like dihadron correlation measurements.

In this work, non-central 20-60% Au+Au collisions at the nucleon-nucleon center of mass energy of $\sqrt{s_{NN}} = 200$ GeV are analysed [9, 10]. As a reference inclusive dihadron correlation data from minimum bias d +Au collisions, which include cold nuclear matter effects, are presented. (The minimum bias d +Au and p + p data are similar [4, 5].) The Au+Au and d +Au data were taken by the STAR experiment at RHIC in 2004 and 2003, respectively. The details of the STAR experiment can be found in Ref. [11]. The main detector used for this analysis is the Time Projection Chamber (TPC) [12], residing in a solenoidal magnet (0.5 Tesla magnetic field along the beam-axis). Events with a primary vertex within ± 30 cm of the TPC center are used. The Au+Au centrality is defined by the measured charged particle multiplicity in the TPC within $|\eta| < 0.5$ [13]. Tracks are used if they are composed of at least 20 hits and 51% of the maximum possible hits and extrapolate to within 2 cm of the primary vertex. The same event and track cuts are applied to particle tracks used for event-plane reconstruction and for the correlation analysis.

Particles with $p_T < 2$ GeV/ c are used to determine the second-order harmonic event plane to ensure good event-plane resolutions. To avoid self-correlations, particles from the p_T bin used in the correlation analysis (e.g., $1 < p_T^{(a)} < 1.5$ GeV/ c) are excluded from EP reconstruction [10]. Nonflow correlations [14], such as dijets, can influence the EP determination. To reduce this effect, particles within $|\Delta\eta| = |\eta - \eta_{\text{trig}}| < 0.5$ from the trigger

particle are excluded from the EP reconstruction in this analysis [10]. This is called the modified reaction-plane (MRP) method [15]. The traditional EP method, on the other hand, does not exclude those particles in the vicinity of the trigger particle in η . Remaining possible biases due to trigger-EP correlations may be estimated by comparing results relative to the EP reconstructed from these two methods. The results are found to be quantitatively similar which suggests that such biases may be small [10].

Dihadron correlations are analyzed for pairs within pseudorapidity $|\eta| < 1$. The trigger particle p_T range is $3 < p_T^{(t)} < 4$ GeV/ c . Two associated particle p_T bins, $1 < p_T^{(a)} < 1.5$ GeV/ c and $1.5 < p_T^{(a)} < 2$ GeV/ c , are analyzed and then added together in the final results. These choices of p_T ranges are motivated by the expectation of significant jet contributions and the need for reasonable statistics [10]. The data are divided into six equal-size slices in ϕ_s and analyzed in azimuthal angle difference ($\Delta\phi$) and pseudorapidity difference ($\Delta\eta$) between associated and trigger particle. The associated particle yields are corrected for single-particle track reconstruction efficiency which is obtained from embedding simulated tracks into real events [16]. The detector non-uniformity in $\Delta\phi$ is corrected by the event-mixing technique, where the trigger particle from one event is paired with associated particles from another event with approximately matching primary vertex position and event multiplicity [5, 10]. The two-particle acceptance in $\Delta\eta$, approximately triangle-shaped, is not corrected for [5]. The correlation function is normalized by the number of trigger particles in its corresponding ϕ_s bin.

Figure 1 shows the raw azimuthal correlations as a function of ϕ_s . A cut of $|\Delta\eta| > 0.7$ is applied on the pseudorapidity difference between the trigger and associated particles in order to minimize the near-side jet contributions [10]. The overall systematic uncertainty on the raw correlation functions is 5%, dominated by that in the efficiency correction.

Particles from the underlying event are uncorrelated with the trigger particle (and the corresponding jet), and follow the non-uniform distribution pattern in $\Delta\phi$ defined by the anisotropic flow. This background has to be removed in order to study jet-like correlations. The major background contribution comes from elliptic flow (v_2). However, quadratic flow (v_4) correlated to ψ_2 can also have a sizable contribution [17]. Due to fluctuations in the initial overlap geometry [8], finite odd harmonic flows, particularly triangular flow (v_3) can also contribute [18]. Such odd harmonics are reproduced in transport models AMPT (A Multi-Phase Transport) [19] and UrQMD (Ultra-relativistic Quantum Molecular Dynamics) [20], as well as in event-by-event hydrodynamic calculations with hot spots [21] or incorporating initial geometry fluctuations [22]. The measured v_3 by both the event-plane and two-particle cumulant methods at RHIC [23, 24] are qualitatively consistent with hydrodynamic calculations.

In this analysis, the flow correlated background is given

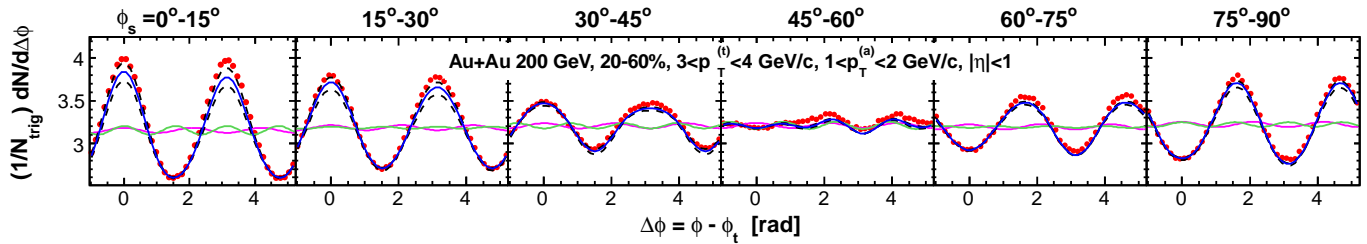


FIG. 1: (Color online) Raw dihadron $\Delta\phi$ correlations (data points) as a function of $\phi_s = |\phi_t - \psi_{\text{EP}}|$, with a cut on the trigger-associated pseudo-rapidity difference of $|\Delta\eta| > 0.7$. The triangle two-particle $\Delta\eta$ acceptance is not corrected. Statistical errors are smaller than the symbol size; systematic uncertainty is 5% (not shown). The curves are flow modulated ZYAM background by Eq. (1) (blue solid), its systematic uncertainty boundaries (dashed), and the v_3 (pink solid) and $v_4\{\psi_2\}$ (green solid) contributions.

116 by [17]

$$\frac{dN}{d\Delta\phi} = B \left(1 + 2v_2^{(a)} v_2^{(t, \phi_s)} \cos 2\Delta\phi + 2v_3^{(a)} v_3^{(t)} \cos 3\Delta\phi + 2v_4^{(a)} \{\psi_2\} v_4^{(t, \phi_s)} \{\psi_2\} \cos 4\Delta\phi + 2V_4\{\text{uc}\} \cos 4\Delta\phi \right). \quad (1)$$

1 Here B is the background normalization (see below); 32
 2 $v_2^{(a)}$ and $v_4^{(a)}\{\psi_2\}$ are the associated particles' second 33
 3 and fourth harmonics with respect to ψ_2 ; and $v_2^{(t, \phi_s)}$ 34
 4 and $v_4^{(t, \phi_s)}\{\psi_2\}$ are the average harmonics of the trigger 35
 5 particles, $v_n^{(t, \phi_s)} = \langle \cos n(\phi_t - \psi_2) \rangle^{(\phi_s)}$, where the aver- 36
 6 ages are taken over the slice around ϕ_s as $\phi_s - \pi/24 < 37$
 7 $|\phi_t - \psi_{\text{EP}}| < \phi_s + \pi/24$. Since the triangularity orienta- 38
 8 tion is random relative to ψ_2 , the triangular flow back- 39
 9 ground is independent of EP, where $v_3^{(t)}$ and $v_3^{(a)}$ are the 40
 10 trigger and associated particle triangular flows. The last 41
 11 term in Eq. (1) arises from v_4 fluctuations uncorrelated 42
 12 to ψ_2 (see below). Higher-order harmonic flows are neg- 43
 13 ligible [10]. 44

14 Eq. (1) does not include the first order harmonic, v_1 . 45
 15 The effect of directed flow, rapidity-odd due to collec- 46
 16 tive sideways deflection of particles, is small and can be 47
 17 neglected [25]. It has been suggested [26] that v_1 fluctua- 48
 18 tion effects (sometimes called rapidity-even v_1) may not 49
 19 be small due to initial geometry fluctuations. Prelimi- 50
 20 nary data [27] indicate that the dipole fluctuation effect 51
 21 changes sign at $p_T \approx 1$ GeV/c, negative at lower p_T and 52
 22 positive at higher p_T . For $p_T^{(a)} = 1-2$ GeV/c used in this 53
 23 analysis, the dipole fluctuation effect is approximately 54
 24 zero and may be neglected. Note that the possible effect 55
 25 of statistical global momentum conservation can gener- 56
 26 ate a negative dipole. However, this is considered as part 57
 27 of the correlation signal, just as momentum conservation 58
 28 by any other mechanisms, for example dijet production. 60

29 The flow correlated background given by Eq. (1) 61
 30 is shown in Fig. 1 as solid curves. The back- 62
 31 ground curves have been normalized assuming that the 63

background-subtracted signal has Zero Yield At Mini-
 mum (ZYAM) [5, 28]. An alternative approach that has
 been used to describe dihadron correlation data treats
 the anisotropic flow modulations as free parameters in
 a multi-parameter model fit to the dihadron correlation
 functions in 2-dimensional $\Delta\eta$ - $\Delta\phi$ space [29]. A detailed
 discussion can be found in Ref. [10].

The major systematic uncertainties on the results re-
 ported here come from uncertainties in the determina-
 tion of the anisotropic flows. Two v_2 measurements
 are used [7]. One is the two-particle cumulant $v_2\{2\}$
 which overestimates elliptic flow due to nonflow contam-
 inations. A major component of nonflow comes from
 correlated pairs at small opening angle [29]. To sup-
 press nonflow, a pseudo-rapidity η -gap (η_{gap}) of 0.7 is
 applied between the particle of interest and the refer-
 ence particle used in the $v_2\{2\}$ measurement. However,
 away-side two-particle correlations, such as those due
 to di-jets, cannot be eliminated. The other measure-
 ment is the four-particle cumulant $v_2\{4\}$ which under-
 estimates elliptic flow because the flow fluctuation effect
 in $v_2\{4\}$ is negative [30]. The range between $v_2\{2\}$ and
 $v_2\{4\}$ is therefore treated as a systematic uncertainty,
 as in Refs. [5], and their average is used as the best
 estimate for v_2 . v_3 and v_4 are obtained by the two-
 particle cumulant method [10, 24] with $\eta_{\text{gap}} = 0.7$, as
 for $v_2\{2\}$. Since $v_3\{2\}$ decreases with $\Delta\eta$ [24], the $v_3\{2\}$
 represents the maximum flow for the correlation func-
 tions at $|\Delta\eta| > 0.7$. The $v_4\{\psi_2\}$ is parameterized [15]
 by $v_4\{\psi_2\} = 1.15v_2^2$. The ψ_2 -uncorrelated $V_4\{\text{uc}\}$ is ob-
 tained as $\sqrt{v_4\{2\}^2 - v_4\{\psi_2\}^2}$, and is found to be negli-
 gible for the 20-60% centrality range used in this anal-

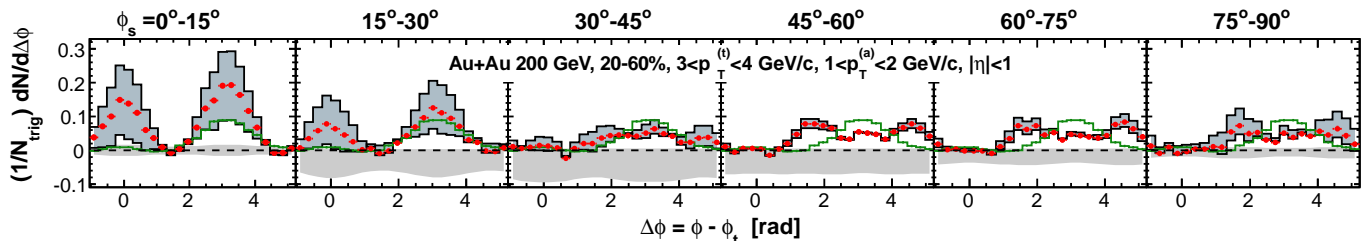


FIG. 2: (Color online) Background-subtracted dihadron $\Delta\phi$ correlations as a function of $\phi_s = |\phi_t - \psi_{EP}|$, with a cut on the trigger-associated pseudo-rapidity difference of $|\Delta\eta| > 0.7$. The triangle two-particle $\Delta\eta$ acceptance is not corrected. Flow background is subtracted by Eq. (1). Systematic uncertainties due to flow subtraction are shown as black histograms enclosing the shaded area; those due to the ZYAM normalization are shown in the horizontal shaded band around zero. Statistical errors are smaller than the point size. For comparison, the inclusive dihadron correlations from d +Au collisions are superimposed as the green histogram with statistical errors.

64 ysis [10]. The v_n values used in the flow background 28
65 subtraction are tabulated in Ref. [10]. 29

66 Another major source of systematic uncertainties 30
1 comes from background normalization by ZYAM. This 31
2 is assessed by varying the size of the normalization range 32
3 in $\Delta\phi$ between $\pi/12$ and $\pi/4$ (default is $\pi/6$), similar to 33
4 what was done in Ref. [5]. The ZYAM assumption likely 34
5 gives an upper limit to the background from the underlying 35
6 event. To estimate this effect, two ZYAM background 36
7 levels are obtained from correlation functions at posi- 37
8 tive $\phi_t - \psi_{EP}$ and negative $\phi_t - \psi_{EP}$ respectively. Those 38
9 ZYAM backgrounds are always lower than the default B 39
10 from ZYAM of the combined correlation function. The 40
11 difference is treated as an additional, one-sided system- 41
12 atic uncertainty on B . The different sources of systematic 42
13 uncertainties on B are added in quadrature. 43

14 Figure 2 shows the background-subtracted dihadron 44
15 correlations as a function of ϕ_s . The black histograms 45
16 enclosing the shaded area indicate the systematic uncer- 46
17 tainties due to anisotropic flow. The horizontal shaded 47
18 band around zero indicates the systematic uncertainties 48
19 due to ZYAM background normalization. For compar- 49
20 ison the minimum-bias d +Au inclusive dihadron corre- 50
21 lation (without differentiating with respect to an “event 51
22 plane”) is superimposed in each panel in Fig. 2. For both 52
23 Au+Au and d +Au, a cut of $|\Delta\eta| > 0.7$ is applied be- 53
24 tween the trigger and associated particles to minimize the 54
25 near-side jet contributions. As seen in Fig. 2, the near- 55
26 side correlations are mostly consistent with zero within 56
27 systematic uncertainties. Previous dihadron correlations 57

without v_3 subtraction have shown a near-side correla-
tion at large $\Delta\eta$ in heavy-ion collisions [5, 31], called the
ridge, suggesting the ridge appears to be mainly due to
 v_3 . However, there appears a finite ridge remaining for
in-plane trigger particles ($\phi_s < 15^\circ$) beyond the maxi-
mum flow subtraction.

Unlike the near side, the away-side correlation is finite
for all ϕ_s . The correlation structure evolves with trigger
particles moving from the in-plane to the out-of-plane di-
rection. The away-side correlation is single peaked, simi-
lar to d +Au results, for in-plane trigger particles and
appears to be significantly broadened or double-peaked
for out-of-plane trigger particles.

The effect of a ϕ_s -dependent v_2 is investigated [10] and
found to eliminate the ridge correlation entirely. How-
ever, the exercise does not reveal the physics mechanism
of the possible ridge because the ϕ_s -dependent v_2 is a
manifestation of a ϕ_s -dependent ridge, and vice versa.
Even with the subtraction of a ϕ_s -dependent v_2 , the
away-side structure remains robust [10]. The possible
bias in event-plane reconstruction by the trigger partic-
le and its associated (away-side) particles is investigated
and is unlikely to be the cause of the observed away-side
structure [10].

To study the structure of the large $\Delta\eta$ correlation func-
tions quantitatively, the data are fit with two away-side
Gaussian peaks symmetric about $\Delta\phi = \pi$, a near-side
Gaussian at $\Delta\phi = 0$ for the ridge, and a back-to-back
Gaussian at $\Delta\phi = \pi$ (referred to as away-side ridge) with
identical width as the near-side ridge [10]. Namely

$$\frac{1}{N_{\text{trig}}} \frac{dN}{d\Delta\phi} = \frac{Y_{AS}}{\sqrt{2\pi}\sigma_{AS}} \left(e^{-\frac{(\Delta\phi - \pi + \theta)^2}{2\sigma_{AS}^2}} + e^{-\frac{(\Delta\phi - \pi - \theta)^2}{2\sigma_{AS}^2}} \right) + \frac{1}{\sqrt{2\pi}\sigma_{\text{ridge}}} \left(Y_{\text{ridge,NS}} e^{-\frac{(\Delta\phi)^2}{2\sigma_{\text{ridge}}^2}} + Y_{\text{ridge,AS}} e^{-\frac{(\Delta\phi - \pi)^2}{2\sigma_{\text{ridge}}^2}} \right), \quad (2)$$

58 where the Gaussians are repeated with period of 2π . The 60
59 magnitudes of the ridge Gaussians are allowed to vary in- 61

dependently according to the data. The fit parameters
are shown in Fig. 3 as a function of ϕ_s . The data points

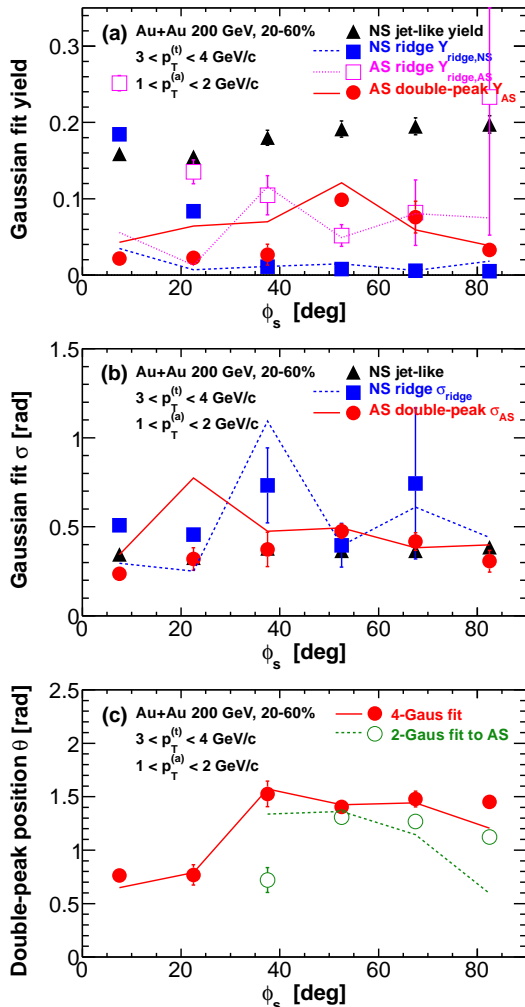


FIG. 3: (Color online) Parameters of four-Gaussian fit to the background subtracted dihadron correlations at $|\Delta\eta| > 0.7$ as a function of ϕ_s . The near-side (NS) jet-like correlation results are also shown; they are obtained by the difference in $\Delta\phi$ correlations at small and large $\Delta\eta$ from Ref. [10]. (a) Correlated yields where the NS jet-like ($|\Delta\eta| < 0.7$) and ridge ($|\Delta\eta| > 0.7$) yields are obtained from bin counting within $|\Delta\phi| < 1$; (b) Gaussian peak widths in $\Delta\phi$; and (c) The away-side (AS) double-peak Gaussian centroid. For comparison the centroid from a two-Gaussian fit to the AS correlation ($|\Delta\phi| > 0.7$) is shown for the four out-of-plane slices. Error bars are statistical only. The curves correspond to the results with maximum flow subtraction by the two-particle cumulant method, which indicate the systematics.

are results with default v_2 subtraction and the curves are the corresponding results with the maximum flow subtraction by the two-particle cumulant $v_2\{2\}$. Both have subtracted the v_3 background using the two-particle cumulant $v_3\{2\}$. The curves, thus, indicate the results with the maximum systematic uncertainty on one side.

Figure 3(a) shows the Gaussian peak areas of the different correlation components. As a comparison, also

shown is the jet-like yield at small $\Delta\phi$ and $\Delta\eta$ obtained by the difference between $\Delta\phi$ correlations at small and large $\Delta\eta$ [10]. The near-side jet-like ($|\Delta\eta| < 0.7$) and ridge ($|\Delta\eta| > 0.7$) yields are obtained from bin counting within $|\Delta\phi| < 1$. The bin counting and the fit results are consistent. Because the jet-like $\Delta\eta$ correlation width is approximately 0.35 (also see Fig. 3(b)), contributions from the tails of the jet-like correlation beyond 0.7 in $\Delta\eta$ are negligible. As seen from Fig. 3(a), the near-side ridge is mostly consistent with zero except in the in-plane direction where a finite ridge beyond the maximum flow systematics seems to be present. The away-side ridge is larger than the near-side ridge at all ϕ_s . The double-peak strength appears to increase with ϕ_s ; for in-plane triggers, where the away-side is single-peaked, there exists a double-peak component if the $\Delta\phi \sim \pi$ region is populated by a Gaussian of the same width as the near-side ridge.

Fig. 3(b) shows the Gaussian fit widths. The widths do not seem to depend on ϕ_s , however, the present systematic uncertainties are large. Fig. 3(c) shows the fitted double-peak Gaussian centroid in filled circles. For the four large ϕ_s bins where the away-side double-peak is observable, the peak location is far removed from π , almost at $\pi/2$ and $3\pi/2$. The away-side correlation can also be well fit by only two Gaussians symmetric about $\Delta\phi = \pi$ (without the back-to-back ridge). The fitted double peak positions for the four out-of-plane slices are shown in open circles. The double-peak correlation structure has been observed before where v_3 contributions were not subtracted [5, 32]. Whether it is an effect of medium excitation by jet-medium interactions over the long away-side pathlength, such as Mach-cone formation [33], remains an open question. There also can be deflection of away-side correlated particles by the collective flow of the medium, especially in the direction perpendicular to the reaction plane [34]. Deflection of correlated particles may have already been seen in three-particle correlations [35] where the diagonal peak is stronger than the off-diagonal peak whereas the unsubtracted v_3 (and possible Mach-cone emission) should yield the same strength for those peaks. However, in jet-hadron correlations where the trigger jet has significantly larger energy than the trigger particle in this analysis, no deflection of associated particles is observed [36].

In summary, dihadron azimuthal correlations at pseudorapidity difference $|\Delta\eta| > 0.7$ are reported by the STAR experiment for trigger and associated particle p_T ranges of $3 < p_T^{(t)} < 4$ GeV/c and $1 < p_T^{(a)} < 2$ GeV/c in non-central 20-60% Au+Au collisions as a function of the trigger particle azimuthal angle relative to the event plane, $\phi_s = |\phi_t - \psi_{EP}|$. Anisotropic v_2 , v_3 , and v_4 flow backgrounds are subtracted using the Zero Yield At Minimum (ZYAM) method, where the maximum flow parameters are obtained from two-particle cumulant measurements with η -gap of 0.7. Minimum-bias d +Au collision data are presented for comparison. The background subtracted dihadron correlations are found to be modified in

Au+Au collisions relative to d +Au; the modification depends on ϕ_s . The near-side ridge previously observed in heavy-ion collisions may be largely due to triangular flow v_3 ; After v_3 subtraction, however, a finite residual ridge may still be present for in-plane trigger particles. The away-side dihadron correlation broadens from in-plane to out-of-plane, and appears to be double-peaked for out-of-plane trigger particles. The trends of the away-side modification may underscore the importance of pathlength-dependent jet-medium interactions, and should help further the current understanding of high-density QCD in relativistic heavy-ion collisions.

We thank the RHIC Operations Group and RCF at BNL, the NERSC Center at LBNL and the Open Sci-

ence Grid consortium for providing resources and support. This work was supported in part by the Offices of NP and HEP within the U.S. DOE Office of Science, the U.S. NSF, the Sloan Foundation, the DFG cluster of excellence ‘Origin and Structure of the Universe’ of Germany, CNRS/IN2P3, STFC and EPSRC of the United Kingdom, FAPESP CNPq of Brazil, Ministry of Ed. and Sci. of the Russian Federation, NNSFC, CAS, MoST, and MoE of China, GA and MSMT of the Czech Republic, FOM and NWO of the Netherlands, DAE, DST, and CSIR of India, Polish Ministry of Sci. and Higher Ed., Korea Research Foundation, Ministry of Sci., Ed. and Sports of the Rep. Of Croatia, Russian Ministry of Sci. and Tech, and RosAtom of Russia.

-
- [1] I. Arsene *et al.* (BRAHMS Collaboration), Nucl. Phys. **A757**, 1 (2005); B. B. Back *et al.* (PHOBOS Collaboration), Nucl. Phys. **A757**, 28 (2005); J. Adams *et al.* (STAR Collaboration), Nucl. Phys. **A757**, 102 (2005); K. Adcox *et al.* (PHENIX Collaboration), Nucl. Phys. **A757**, 184 (2005).
- [2] U. Heinz and P. F. Kolb, Nucl. Phys. **A702**, 269 (2002).
- [3] X.-N. Wang and M. Gyulassy, Phys. Rev. Lett. **68**, 1480 (1992).
- [4] S. Adler *et al.* (PHENIX Collaboration), Phys. Rev. Lett. **91**, 072301 (2003); J. Adams *et al.* (STAR Collaboration) Phys. Rev. Lett. **91**, 072304 (2003); C. Adler *et al.* (STAR Collaboration), Phys. Rev. Lett. **90**, 082302 (2003).
- [5] J. Adams *et al.* (STAR Collaboration), Phys. Rev. Lett. **95**, 152301 (2005); M. M. Aggarwal *et al.* (STAR Collaboration), Phys. Rev. C **82**, 024912 (2010).
- [6] J. Adams *et al.* (STAR Collaboration), Phys. Rev. Lett. **93**, 252301 (2004).
- [7] A. M. Poskanzer and S. A. Voloshin, Phys. Rev. C **58**, 1671 (1998).
- [8] B. Alver *et al.*, Phys. Rev. C **77**, 014906 (2008).
- [9] Aoji Feng, ‘‘Di-hadron Azimuthal Correlations Relative to Reaction Plane in Au + Au Collisions at $\sqrt{s_{NN}} = 200$ GeV’’, Ph.D. thesis, Institute of Particle Physics, CCNU, May 2008; Joshua Konzer, ‘‘Jet-Like Dihadron Correlations in Heavy Ion Collisions’’, Ph.D. thesis, Purdue University, July 2013.
- [10] H. Agakishiev *et al.* (STAR Collaboration), arXiv:1010.0690.
- [11] K. H. Ackermann *et al.* (STAR Collaboration), Nucl. Instrum. Meth. **A499**, 624 (2003).
- [12] K. H. Ackermann *et al.* (STAR Collaboration), Nucl. Phys. **A661**, 681 (1999).
- [13] J. Adams *et al.* (STAR Collaboration), Phys. Rev. Lett. **92**, 112301 (2004).
- [14] N. Borghini, P. M. Dinh and J. Y. Ollitrault, Phys. Rev. C **62**, 034902 (2000).
- [15] J. Adams *et al.* (STAR Collaboration), Phys. Rev. C **72**, 014904 (2005).
- [16] B. I. Abelev *et al.* (STAR Collaboration), Phys. Rev. C **79**, 034909 (2009).
- [17] J. Bielcikova *et al.*, Phys. Rev. C **69**, 021901(R) (2004); J. Konzer and F. Wang, Nucl. Instrum. Meth. **A606**, 713 (2009).
- [18] A. P. Mishra *et al.*, Phys. Rev. C **77**, 064902 (2008); B. Alver and G. Roland, Phys. Rev. C **81**, 054905 (2010), Erratum-ibid. C **82**, 039903 (2010).
- [19] J. Xu and C. M. Ko, Phys. Rev. C **84**, 014903 (2011).
- [20] H. Petersen *et al.*, Phys. Rev. C **82**, 041901 (2010).
- [21] J. Takahashi *et al.*, Phys. Rev. Lett. **103**, 242301 (2009); R. P. G. Andrade *et al.*, Phys. Lett. **B712**, 226 (2012); W. L. Qian *et al.*, Phys. Rev. C **87**, 014904 (2013).
- [22] B. Schenke, S. Jeon and C. Gale, Phys. Rev. Lett. **106**, 042301 (2011); Z. Qiu and U. W. Heinz, Phys. Rev. C **84**, 024911 (2011); H. Song *et al.*, Phys. Rev. Lett. **106**, 192301 (2011); B. Schenke, S. Jeon and C. Gale, Phys. Rev. C **85**, 024901 (2012); B. Schenke, P. Tribedy and R. Venugopalan, Phys. Rev. Lett. **108**, 252301 (2012).
- [23] A. Adare *et al.* (PHENIX Collaboration), Phys. Rev. Lett. **107**, 252301 (2011).
- [24] L. Adamczyk *et al.* (STAR Collaboration), Phys. Rev. C **88**, 014904 (2013).
- [25] B. I. Abelev *et al.* (STAR Collaboration), Phys. Rev. Lett. **101**, 252301 (2008).
- [26] D. Teaney and L. Yan, Phys. Rev. C **83**, 064904 (2011).
- [27] Y. Pandit (STAR Collaboration), J. Phys. Conf. Ser. **446**, 012012 (2013).
- [28] N. N. Ajitanand *et al.*, Phys. Rev. C **72**, 011902 (2005).
- [29] G. Agakishiev *et al.* (STAR Collaboration), Phys. Rev. C **86**, 064902 (2012).
- [30] C. Adler *et al.* (STAR Collaboration), Phys. Rev. C **66**, 034904 (2002).
- [31] B. I. Abelev *et al.* (STAR Collaboration), Phys. Rev. C **80**, 064912 (2009); B. I. Abelev *et al.* (STAR Collaboration), Phys. Rev. Lett. **105**, 022301 (2010).
- [32] S. S. Adler *et al.* (PHENIX Collaboration), Phys. Rev. Lett. **97**, 052301 (2006); A. Adare *et al.* (PHENIX Collaboration), Phys. Rev. C **78**, 014901 (2008).
- [33] H. Stoecker, Nucl. Phys. **A750**, 121 (2005); J. Casalderrey-Solana, E. V. Shuryak, and D. Teaney, J. Phys. Conf. Ser. **27**, 22 (2005); J. Ruppert and B. Müller, Phys. Lett. **B618**, 123 (2005).
- [34] B. Betz *et al.*, Phys. Rev. Lett. **105**, 222301 (2010); G. L. Ma and X. N. Wang, Phys. Rev. Lett. **106**, 162301

- 114 (2011).
115 [35] B. I. Abelev *et al.* (STAR Collaboration),
116 Phys. Rev. Lett. **102**, 052302 (2009).
- 1 [36] L. Adamczyk *et al.* (STAR Collaboration),
2 arXiv:1302.6184.